Journal Pre-proofs

Poly(DL-lactic acid) scaffolds as a bone targeting platform for the co-delivery of antimicrobial agents against *S. aureus-C. albicans* mixed biofilms

M. Zegre, J. Barros, I.A.C. Ribeiro, C. Santos, L.A. Caetano, L. Gonçalves, F.J. Monteiro Resource, M.P. Ferraz, A. Bettencourt

PII: S0378-5173(22)00387-8
DOI: https://doi.org/10.1016/j.ijpharm.2022.121832
Reference: IJP 121832

To appear in: *International Journal of Pharmaceutics*

Received Date: 10 February 2022
Revised Date: 11 May 2022
Accepted Date: 12 May 2022

Please cite this article as: M. Zegre, J. Barros, I.A.C. Ribeiro, C. Santos, L.A. Caetano, L. Gonçalves, F.J. Monteiro Resource, M.P. Ferraz, A. Bettencourt, Poly(DL-lactic acid) scaffolds as a bone targeting platform for the co-delivery of antimicrobial agents against *S. aureus-C. albicans* mixed biofilms, *International Journal of Pharmaceutics* (2022), doi: https://doi.org/10.1016/j.ijpharm.2022.121832

Poly(DL-lactic acid) scaffolds as a bone targeting platform for the co-delivery of antimicrobial agents against *S. aureus*-*C. albicans* mixed biofilms

M. Zegre[a,b#], J. Barros[c,d#], I.A.C. Ribeiro[a], C. Santos[e,f], L. A. Caetano[a,b], L. Gonçalves[a], F.J. Monteiro[c,d,g], M.P. Ferraz[c,d,g*], A. Bettencourt[a*]

[a]Research Institute for Medicines (iMed.ULisboa), Faculdade de Farmácia, Universidade de Lisboa, Av. Prof. Gama Pinto, 1649-003, Lisboa, Portugal.
[b]H&TRC – Centro de Investigação em Saúde e Tecnologia, ESTeSL – Escola Superior de Tecnologia da Saúde de Lisboa, IPL – Instituto Politécnico de Lisboa, Av. D. João II, Lote 4.69.01, 1990-096, Lisboa, Portugal.
[c]i3S – Instituto de Investigação e Inovação em Saúde – Associação, Universidade do Porto, R. Alfredo Allen 208, 4200-135, Porto, Portugal.
[d]INEB – Instituto de Engenharia Biomédica, Universidade do Porto, R. Alfredo Allen 208, 4200-135, Porto, Portugal.
[e]CQE - Instituto Superior Técnico, Universidade de Lisboa, Av. Rovisco Pais 1049-001, Lisboa, Portugal.
[f]EST Setúbal, CDP2T, Instituto Politécnico de Setúbal, Campus IPS, 2910 Setúbal, Portugal.
[g]FEUP/DEMM – Departamento de Engenharia Metalúrgica e de Materiais, Faculdade de Engenharia da Universidade do Porto, 4200-465 Porto, Portugal.

# co-first author, both authors contributed equally to the work

*Corresponding author: M.P. Ferraz, i3S – Instituto de Investigação e Inovação em Saúde – Associação, Universidade do Porto, R. Alfredo Allen 208, 4200-135, Porto, Portugal. Tel:+351 226 074 900; e-mail address: mpferraz@ineb.up.pt

*Corresponding author: A. Bettencourt, Research Institute for Medicines (iMed.ULisboa), Faculdade de Farmácia, Universidade de Lisboa, Avenida Prof. Gama Pinto, 1649-003, Lisboa Portugal. e-mail address: asimao@ff.ulisboa.pt

ABSTRACT

New strategies for the treatment of polymicrobial bone infections are required. In this study, the co-delivery of two antimicrobials by poly(D,L-lactic acid) (PDLLA) scaffolds was investigated in a polymicrobial biofilm model. PDLLA scaffolds were prepared by solvent casting/particulate leaching methodology, incorporating minocycline and voriconazole as clinically relevant antimicrobial agents. The scaffolds presented a sponge-like appearance, suitable to support cell proliferation and drug release. Single- and dual-species biofilm models of *Staphylococcus aureus* and *Candida albicans* were developed and characterized. *S. aureus* presented a higher ability to form single-species biofilms, compared to *C. albicans*. Minocycline and voriconazole-loaded PDLLA scaffolds showed activity against *S. aureus* and *C. albicans* single- and dual-biofilms. Ultimately, the cytocompatibility/functional activity of PDLLA scaffolds observed in human MG-63 osteosarcoma cells unveil their potential as a next-generation co-delivery system for antimicrobial therapy in bone infections.

Keywords: bone infection, polymicrobial biofilms, minocycline, voriconazole, co-delivery, localized antibiotic delivery

Abbreviations: PDLLA, poly(D,L-lactic acid); Min, minocycline; Vor, voriconazole; MG-63, human osteoblast-like cells; GMP, Good Manufacturing Practices

GRAPHICAL ABSTRACT

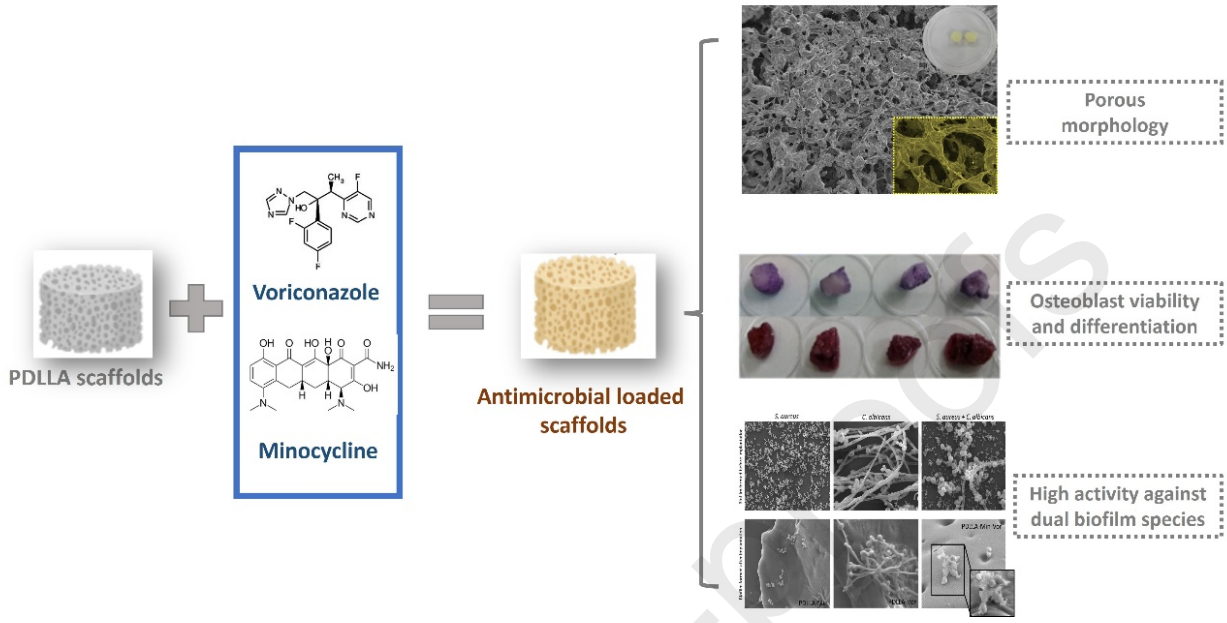

1. Introduction

The treatment of bacterial joint and bone infections in patients after multiple revision arthroplasties is very challenging. (Enz et al., 2021) Also, with the increasing occurrence of factors predisposing to candidemia, candida osteomyelitis is being diagnosed more frequently. (Lerch et al., 2003) The occurrence of opportunistic polymicrobial infections is a further detrimental factor that complicates these infections. (Enz et al., 2021) In fact, an increasing number of studies report the co-isolation of bacterial and fungal species, such as *Staphylococcus aureus* and *Candida albicans,* from polymicrobial biofilm associated with bone infections (e.g. prosthetic joint infections, osteomyelitis) and/or infections related to indwelling medical devices. (Enz et al., 2021; Lerch et al., 2003; Li et al., 2020a; Peters et al., 2012; Zago et al., 2015) Microorganisms can interact in a synergistic or inhibitory way, impacting the efficiency of the treatment strategy and the disease outcome. (Van Dyck et al., 2021a)

In the quest for novel therapeutic strategies, recent studies show that site-specific drug delivery scaffolds with high efficiency to specific sites and low toxicity as compared to systemic and oral administration routes can significantly reduce the number of viable microorganisms either in mono- or polymicrobial-biofilms and prevent the development of infection in bone disease. (Beenken et al., 2021; Flurin et al., 2021) Dual/co-delivery strategies are being tested for bone tissue engineering (Farokhi et al., 2016), such as for the release of angiogenic and osteogenic peptides (Wang et al., 2021) to improve bone regeneration with enhanced vascularization. The association of an antibiotic (vancomycin) and growth factors to prevent infection and stimulate healing in large bone injuries has also been explored. (Doty et al., 2014; Li et al., 2013)

Noteworthy, the development of co-delivery systems of at least two antimicrobials is yet an overlooked approach, (McLaren et al., 2014; Van Dyck et al., 2021b) while it

may be a critical strategy for the treatment of infections associated with polymicrobial biofilms. (Fanaei Pirlar et al., 2020; Harriott and Noverr, 2009; Qu et al., 2016) Concomitantly, it is recommended to assess the contribution of each microbial population within biofilm in order to select the best therapy to treat polymicrobial infections.

Among different biomaterials used for scaffold drug-deliver matrices, poly (lactic acid) (PLA) based polymers are being widely studied due to their versatility, low toxicity and tailored biodegradability having the US Food and Drug Administration (FDA) approval for clinical use. (DeStefano et al., 2020; Xiao et al., 2012) PLA can be seen as a "family" of polymers, which include the homopolymers PLLA and PDLA (synthesized from mixtures of pure L- or D-lactic acid) and the copolymer PDLLA (obtained from the racemic mixture). (DeStefano et al., 2020) In particularly, due to the amorphous nature of PDLLA, this polymer presents a faster and more controllable in vivo degradation profile than the semicrystalline PLLA and PDLA, which can be advantageous for drug delivery and bone regeneration purposes. (Silva et al., 2017; Xiao et al., 2012)

The adequate osteoconductive and anti-*S. aureus* effects of a collagen-functionalized PDLLA porous scaffold loaded with minocycline (a tetracycline antibiotic) have been previously demonstrated by our group. (Martin et al., 2019a) Specifically, these types of scaffolds were primarily designed for drug delivery purposes and not for load-bearing applications due to PDLLA well-known poor stiffness and compression strength. (Mouriño and Boccaccini, 2010) In the present study, we focus on the problem of mixed bacterial- fungal biofilm infections and the joining of two antimicrobials in the PDLLA scaffold. Minocycline (a tetracycline broad-spectrum antibiotic) and voriconazole (an antifungal triazole) were the chosen model drugs. (Du et al., 2017; Miller et al., 2013;

Tan et al., 2021) Importantly, minocycline may represent a promising drug that can be administered in combination with azoles (namely voriconazole) to treat infections caused by pathogenic Candida species. (Tan et al., 2021) Morphological and chemical properties of the co-delivery PDLLA scaffolds, as well as drug release profiles, were examined. The antibiofilm activity of the co-delivery PDLLA scaffolds was tested against single- and dual-species biofilms of *S. aureus* and *C. albicans*. The formation of dual-species *S. aureus – C. albicans* biofilms was studied over time to determine the time needed to reach a mature biofilm and to understand the relationship between both microorganisms during *in vitro* biofilm formation. Cytocompatibility and osteoconductive tests were also conducted using MG-63 osteoblasts to assess the potential of co-delivery PDLLA scaffolds for bone regeneration.

2. Materials and Methods

2.1. Materials

Poly-DL-lactic acid (PURASORB®, Corbion), average M_w obtained by GPC of 76,000 g/mol is a GMP grade copolymer (50% of isomer D and 50% of isomer L) with an inherent viscosity midpoint of 0.6 dL/g. Other materials were dichloromethane (Sigma Aldrich), sodium chloride (Honeywell, Fluka), collagen hydrolysate type I fibrillar (kindly donated by Dra Mădălina Kaya from Department of Collagen Research, Romania), ethanol anhydrous (Carlo Erba), minocycline hydrochloride (kindly donated by Atral Cipan, Portugal), voriconazole (Glentham Life Sciences).

2.2. Scaffolds fabrication

Porous PDLLA scaffolds (10×10×10 mm) were prepared by solvent casting/particulate leaching method previously optimized in our laboratories. (Martin et al., 2019a) Dichloromethane (DCM) was used as polymer solvent and sodium chloride (250-500

μm) as porogen. PDLLA (200 mg) dissolved in DCM (400 mg/mL) was mixed with the salt (1.78 g). The mixture was packed into a cubic silicon mold (10×10×10mm) and the samples were placed in a desiccator at 25°C for 24 h, to eliminate the DCM. Afterwards, scaffolds were placed in distilled water for 48 h (the water was replaced after the first 24 hours) under magnetic stirring to leach out the salt particles (confirmed by conductivity assessment using a conductivity meter apparatus XS Instruments, Italy; acceptable value less than 1 μS/cm at 25 C). Sterilization of the scaffolds was obtained by immersion in ethanol 70% (V/V) for 24 h, right after the leaching of the salt particles. Subsequently, all the scaffolds were immersed in an adsorption aqueous solution containing 7.5 mg/mL of collagen at room temperature at 200 rpm under mixing for 24 h. Additionally, one group was also adsorbed with 0.1 mg/mL of minocycline (PDLLA-Min), another one with 0.1 mg/mL of voriconazol (PDLLA-Vor) and a third group (PDLLA-Min-Vor) with an aqueous solution containing both drugs with the same concentration (0.1 mg/mL). All scaffolds were dried in a desiccator for at least 48 h. Samples functionalized only with collagen (PDLLA) were used as controls.

2.3. Scaffolds characterization

2.3.1. Physical-chemical analysis

The morphological features (including porous size) of the obtained scaffolds were examined using a field emission gun scanning electron microscope (FEG-SEM; JEOL-JSM7001F). A thin layer of conductive gold-palladium (Quorum Technologies Q150T ES sputter coater) was coated to increase the conductivity of the scaffolds.

2.3.2. Chemical composition

Fourier transform infrared spectroscopy-attenuated total reflection (FTIR-ATR) analysis was performed using a Nicolet 5700 (Thermo Electron) spectrometer for chemical

analysis of the scaffolds. For FTIR-ATR measurements, all scaffolds were placed on the ATR diamond crystal, and the spectra obtained in the range of 600 to 4000 cm^{-1} resulted from an average of 128 scans collected with a resolution of 8 cm^{-1}.

2.3.3. Drug loading and Release Studies

Drug loading was determined by quantifying the drugs in the supernatants (non-adsorbed antimicrobials) obtained after scaffold preparation. Minocycline was determined spectrophotometrically at 350 nm (FLUOstar Omega, BMG Labtech). (Martin et al., 2019b) Voriconazole was quantified by a reversed-phase high performance liquid chromatography (RP-HPLC) method in a Shimadzu System (Shimadzu Corporation, LC-6A) coupled to an autosampler (Waters 717plus Autosampler) and a thermostatic column compartment (Dionex STH 585 Column Oven). A LiChrospher® 100 RP-18 analytical column (125 mm × 4 mm, 5 μm particle size, LiChroCART®Merck, Darmstadt, Germany) was used at 30ºC and an isocratic elution was achieved with an acetonitrile-water (3:2) mobile phase. Detection was set at 256 nm, the flow rate was 1 mL/min and the injection volume was 20 μL (Babu and Raju, 2007; Üstündağ Okur et al., 2016)

Each sample was measured three times and the supernatants from antibiotic-free scaffolds were also analyzed and used as control. Drug loading (%DL) was calculated as the percentage of the drug in the scaffolds reported to their weight. (Ferreira et al., 2015; Matos et al., 2015b) All results are displayed as mean ± standard deviation (SD).

Release studies were carried out by submerging each scaffold in a 50 mL Falcon tube with 5 mL of HEPES buffer (VWR Chemicals) 10 mM at pH 7.4 in a shaking water-bath (Memmert) at 37 °C. At predetermined time intervals throughout a 120 h (5 days) period, aliquots of the supernatant were collected and analyzed in triplicate. The

withdrawn aliquots were then replaced with equal volumes of fresh release solution and the medium was changed after the first 96 h. The drugs were assayed as detailed above with respect to drug loading. Further, the released solutions at 6, 24 and 48h were tested in microbiological assays.

2.4. Biofilm formation testing

2.4.1. Microbial Growth and Standardization

S. aureus ATCC 49230 and *C. albicans* ATCC 10231 were used as reference strains. Tryptic Soy Broth (TSB) (Merck Millipore, Germany), Tryptic Soy Agar (TSA) (Merck Millipore, Germany), Manitol Salt Agar (MSA) (Liofilchem, Italy), Sabouraud 2% Dextrose Agar (SDA) (Merck Millipore, Germany) and 0.9% NaCl (Merck Millipore, Germany) were prepared according to the manufacturer's instructions. TSA plates were used to quantify the total cultivable cells (both *S. aureus* and *C. albicans*), whereas MSA and SDA plates were used to selectively quantify the viable *S. aureus* and *C. albicans* strains, respectively. Prior to each experiment, microorganisms were cultured in TSB for 24 h at 37 ºC and 150 rpm. Following incubation, the initial suspensions (at exponential phase) at 1×10^6 Colony-Forming Units (CFU) mL^{-1} of each microorganism were prepared in fresh TSB to be used in the following sections.

2.4.2. Single- and Dual-species biofilm formation

For single-species biofilms, one mL of *S. aureus* or *C. albicans* at 1×10^6 CFU mL^{-1} was added to 24-well tissue culture plates (TCPs), while for dual-species *S. aureus–C. albicans* biofilms, 500 µL cultures of each culture with an initial concentration of 2×10^6 CFU mL^{-1} were used. To induce the microorganism's adherence, the TCPs were incubated for 2 hours at 37°C and 150 rpm. Following incubation, the wells were

carefully rinsed twice with 0.9 % NaCl, to remove planktonic and weakly attached cells, and then fresh TSB medium (1 mL) was added to wells'-adhered biofilms. The TCPs were incubated for 24, 48 and 72 h at 37°C and 150 rpm, to select the time needed to reach a mature biofilm. After each time of incubation, the wells-formed biofilms were rinsed twice with NaCl 0.9% (w/V), removing non-adherent and weakly-adherent microorganisms, and one mL of PBS was added to each well. Then, the TCPs were sonicated for 15 minutes using an ultrasonic water-bath (Transsonic 420, 70 W, 35 kHz, ELMA), to dislodge sessile microorganisms. The sessile populations were quantified by the Colony-Forming Units' (CFUs) method. Microorganism-free wells were used as a negative control.

2.4.3. Single and dual-species biofilms morphology and structures

The biofilms' morphologies and structures were assessed through Scanning Electron Microscopy (SEM). Briefly, single- and dual-species biofilms were formed on Thermanox coverslips (Fisher Scientific, 13 mm diameter, Loughborough, UK) for 72 h, as previously described. Then, pre-washed samples were initially fixed for 30 minutes with 1.5 % glutaraldehyde (Sigma-Aldrich) and then slowly dehydrated in a gradient ethanol series for 15 minutes each. Samples were subsequently dried in a gradient series of hexamethyldisilazane (HMDS, Sigma-Aldrich) solutions for 15 minutes each. The samples were then sputter-coated (SPIModule) with a thin gold/palladium film and analyzed by SEM using a FEI Quanta 400FEG/ESEM microscope (FEI, USA) (Accelerating Voltage: 15 kV). For each sample, five fields were randomly chosen to eliminate possible uneven microorganisms' distribution, with magnifications between 5000 and 15000×.

2.4.4. Antibiofilm activity of the scaffolds (direct effect)

The antibiofilm activity of the scaffolds against single- and dual-species biofilm formation was evaluated following the previous procedure as referred to in 2.4.2, with some modifications. Briefly, scaffolds (PDLLA, PDLLA-Min, PDLLA-Vor, and PDLLA-Min-Vor) and fresh TSB medium (without microorganisms, 1 mL) were added to pre-washed wells-adhered microorganisms. Then, the plates were incubated for 24 h at 37°C and 150 rpm, to form the single- and dual-species biofilms. After incubation, sessile microorganisms were dislodged from wells, and cell densities for either biofilm were quantified by the CFUs method. PDLLA scaffolds and microorganism- free wells were used as positive and negative controls, respectively.

2.4.5. Antibiofilm activity of the scaffolds (released solutions effect)

The sensitivity of single- and dual-species biofilm formation to solutions released from scaffolds (PDLLA, PDLLA-Min, PDLLA-Vor, and PDLLA-Min-Vor) at 6, 24 and 48 h (2.3.3.) was assessed. Briefly, 200 µl of fresh TSB medium supplemented with solutions released from scaffolds (1:1 ratio) were added to pre-washed single- and dual-species biofilms and incubated at 37 °C for 24 h. Consequently, the sessile populations were quantified through the CFUs method. Solution released from PDLLA scaffolds and microorganism-free medium were used as positive and negative controls, respectively.

2.5. Cytocompatibility and functional activity testing

The cytocompatibility and functional activity of PDLLA scaffolds was evaluated with a human osteoblast cell line (MG-63, ATCC®CRL-1427™). The osteoblasts were grown in RPMI 1640 culture medium (Life Technologies, UK), enriched with 10% fetal serum bovine (Life Technologies, UK), 100 units/mL of penicillin G (sodium salt) (Life

Technologies, UK), 100 units/mL of streptomycin sulfate (Life Technologies, UK) and 2 mM L-glutamine (Life Technologies, UK), at 37 ºC, 5 % CO_2 and 99 % humidity. When the cells reached 80 % confluency, they were trypsinized and subcultured at 2×10^5 cells/mL

2.5.1. Cell proliferation

Cell proliferation studies were conducted by fluorometric procedure (AlamarBlue® assay) that correlates directly with the metabolic viable cell number. (Martin et al., 2019a). Dry scaffolds were inoculated with a cell density of 2×10^5 cells/mL, each scaffold with 500 µL. To perform the assay, cells were cultured with the 4 groups of scaffolds up to 28 days in a 24-well plate (non-treated surface, Costar® Merck, Portugal) at 37 °C and 5 % CO_2. The assay was performed once a week; the seeded scaffolds were changed to an empty well with new medium and incubated in AlamarBlue® solution at 37 °C for 2 hours. Resorufin fluorescence was measured in the cell media supernatants (wavelengths of 530 nm for excitation and 590 nm for emission) by microplate reader (FLUOstar Omega, BMGLabtech, Germany).

2.5.2. Alkaline phosphatase (ALP) activity

The ALP activity of MG-63 cells seeded on the scaffolds (during 28 days) was carried out using the BCIP/NBT (5-Bromo-4-chloro-3-indolyl phosphate/Nitro blue tetrazolium) test (Sigma-Aldrich, Spain). (Martin et al., 2019a) In brief, the scaffolds containing the cells were washed twice with sodium chloride solution (0.9 %) and immersed in 700 µL of BCIP-NBT salt solution (for 30 minutes at 37 ºC). Afterwards, photos of the stained scaffolds were recorded. Further, for quantitative evaluation, the scaffolds were changed to an empty eppendorf with 700 µL of 10 % SDS-0.5N HCl to

dissolve the formed precipitate, and incubated at 37 ºC for 30 min, followed by maceration and vortexing, in order to intensify the dissolution process. Aliquots were assembled and the absorbance was measured at 495 nm wavelength by a microplate reader (FLUOstar Omega, BMGLabtech, Germany).

2.5.3. Matrix mineralization

The calcium deposits in the cellular matrix were evaluated through the Alizarin Red assay (VitroView™ Alizarin Red Stain Kit, GeneCopoeia, Inc., USA). After 28 days of inoculation of MG-63 cells, the scaffolds were washed thrice with PBS (Sigma-Aldrich, Spain), followed by sterile water. A volume of Alizarin Red solution was added to the scaffolds (30 minutes at room temperature). After incubation, the samples were washed several times with sterile purified water under agitation. For qualitative evaluation, photos were recorded. To perform the quantitative assay, 5 % SDS-0.5 N HCl (AppliChem GmbH, Germany) solution was added for calcified mineral extraction, followed by an overnight period of incubation at room temperature. Absorbance (wavelength of 405 nm) and fluorescence (wavelengths of 530 nm for excitation and 590 nm for emission) were determined using a microplate reader (FLUOstar Omega, BMGLabtech, Germany).

2.6. Statistical analysis

Regarding drug loading results, the statistical analysis between single delivery *versus* co-delivery system was performed by applying the unpaired Student's t test. One-way analysis of variance (ANOVA) and Tukey HSD multiple comparison *post hoc* test were applied to the microbiological experiments. In the cytocompatibility assessment, the normality of the data was determined by the Shapiro-Wilk test. As non-normal

distributed datasets were found, the Kruskal-Wallis test followed by multiple comparisons using Dunn's test, was performed.

The statistical analysis of all the results was performed using SPSS software (IBM® version 20.0) or GraphPad Prism 5 software v.5.03 (GraphPad Software, San Diego, California, USA). Differences were considered statistically significant at a $p < 0.05$.

3. Results and Discussion

3.1. Morphology, porosity and chemical characterization of the scaffolds

Optical and SEM images of the four groups of scaffolds (PDLLA, PDLLA-Min, PDLLA-Vor, and PDLLA-Min-Vor) are shown in Fig.1. All scaffolds had high porosity and a sponge-like appearance, with differences in color between them: samples with minocycline (PDLLA-Min and PDLLA-Min-Vor) had a yellowish color (Fig. 1A), while the samples PDLLA and PDLLA-Vor had a whitish color typical of the PDLLA (Fig. 1A).

SEM images (Fig. 1A) provide a qualitative appreciation of the porous morphology and size of the developed scaffolds' 3D-structure. In general, all samples presented an open and well-structured porous network composed of interconnected spherical macropores, with micropores in the macropore pore walls (Fig. 1A) that can support cell proliferation and nutrition. (Obayemi et al., 2020) It can be seen that the macropores of the scaffolds were quite uniform and had a pore size of (~200-300 μm) similar to the size of the salt particles. The micropores observed in the pore walls ranged in size from 20 μm to 100 μm (Fig. 1A), which suggests that they were caused by the drying of the solvent during scaffolds' preparation. This type of pore architecture is typical of polymeric scaffolds prepared by the solvent casting/particulate leaching method. (Martin et al., 2019a) Interestingly enough, all groups showed the particularity of also

exhibiting a toughed surface related to collagen fibrils (arrows in Fig. 1A). The interconnected porosities, along with the bioactive role of collagen, evidence scaffolds' optimal structure to ensure the movement of biological fluid, adherence and proliferation of osteoblasts along with appropriateness to local antibiotic delivery. (Sreeja et al., 2020) When comparing with pristine scaffolds, the drug loading does not appear to affect the porous network structure of the described polymeric scaffold.

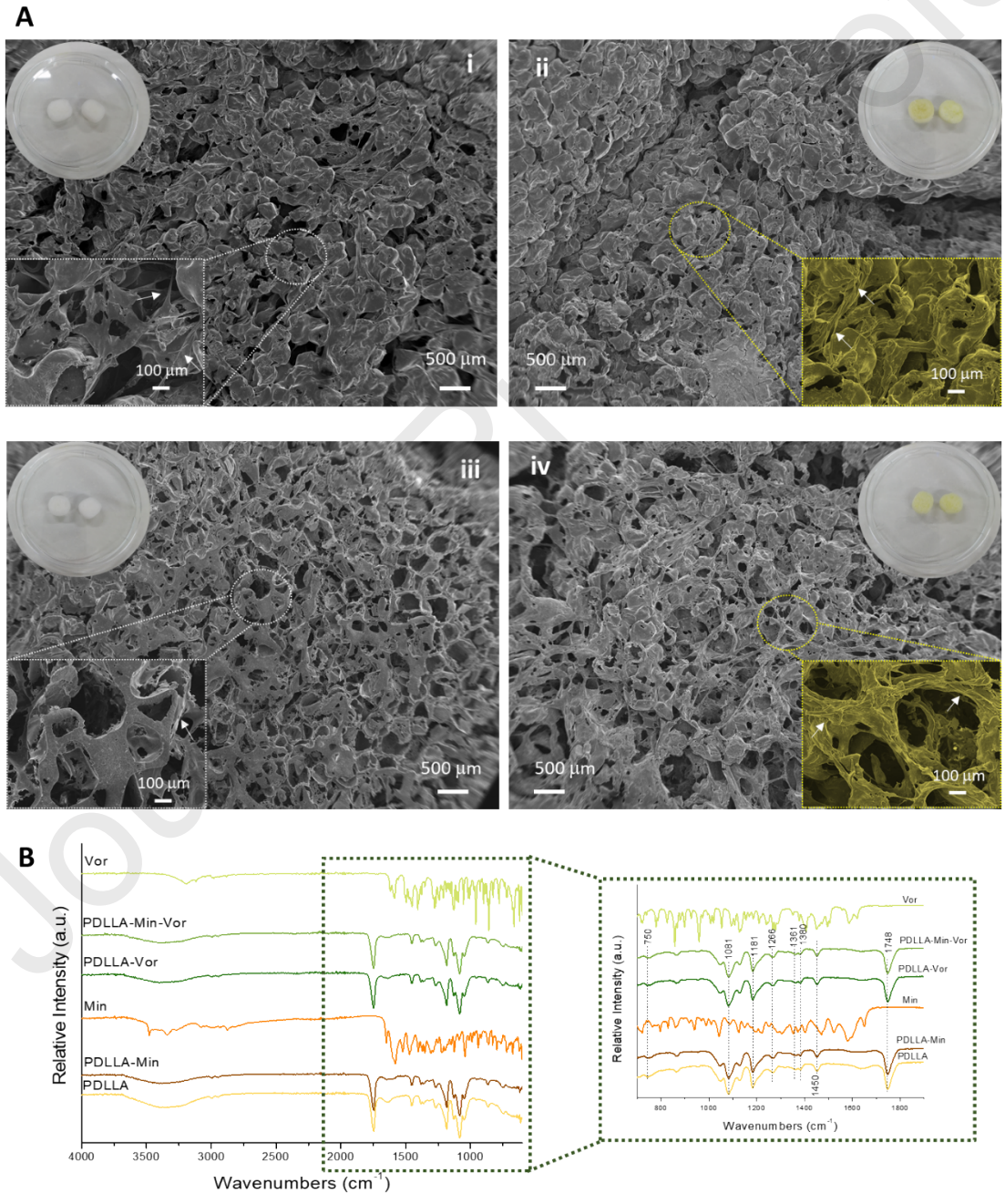

Figure 1. Representative optical images and SEM micrographs (A) of the PDLLA scaffolds (i) with different compositions (PDLLA-Min (ii); PDLLA-Vor (iii) and PDLLA-Min-Vor (iv)) showing in detail the morphological and structural features of the scaffolds (inset images). With the inset white arrow pointing at the collagen fibres; Fourier transform infrared spectroscopy-attenuated total reflection (FTIR-ATR) (B) of PDLLA scaffold, drug loaded scaffolds with Min (PDLLA-Min), pure minocycline (Min), drug loaded scaffolds with Vor (PDLLA-Vor), Vor and Min (PDLLA-Min-Vor) and pure voriconazole (Vor).

Figure 1B shows the FTIR-ATR spectra of pure minocycline, pure voriconazole, pristine and drug-loaded scaffolds. The characteristic absorption bands of PDLLA at 750 cm^{-1} (related with CH vibration), 1081 and 1266 cm^{-1} (=C-O stretching mode of the carboxyl groups), 1181 cm^{-1} (C-C bond), 1361 and 1380 cm^{-1} (CH_2 wagging), 1450 cm^{-1} (CH_3 bending), 1748 cm^{-1} (C=O stretching mode of carbonyl groups), 2940 cm^{-1} (CH_3 asymmetric axial deformation of C-H bonds) and 2994 cm^{-1} (symmetric CH_2 deformation of C-H bonds) (Leal et al., 2019), were observed in all scaffold spectra, indicating that drugs did not induce structural changes on the PDLLA. Moreover, this result indicates that the drugs are physically adsorbed on the scaffolds, which can be an advantage for the release process.

3.2. Drug loading and release studies

The scaffolds showed moderate capacity to be loaded with the selected drugs. Drug loading content (wt%) was calculated as the drug:polymer ratio. The loading of both drugs in the co-delivery system was not significantly different ($p > 0.05$) compared to the single loading ($2.3\pm0.0\times10^{-3}$ *versus* $2.5\pm0.2\times10^{-3}$ % for minocycline, and $4.8\pm0.1\times10^{-3}$ *versus* $4.3\pm0.7\times10^{-3}$ % for voriconazole). The DL low range values

probably reflect the hydrophobic nature of the PDLLA polymer and it´s relative low capacity for water adsorption. (Yang et al., 2018)

With respect to drug release profiles (Fig. 2), immediately after placing the scaffolds in the release media, an initial large bolus of drug was released. This phenomenon is typically referred to as the "burst phase" leading to a higher initial drug delivery. (Huang and Brazel, 2001) In addition, a significant amount of the drug was released within the first 24 hours, which may have a positive impact on infection control on the first day after implantation. (Babaei et al., 2019)

In particular, it is significant that only after a 30 minute period the PDLLA-Min scaffolds delivered a minocycline concentration above the MIC_{90} value for methicillin-susceptible *S. aureus* (MSSA) (4 μg mL^{-1}) and above the MIC_{50} value for methicillin-resistant *S. aureus* (MRSA) (2 μg mL^{-1}). (Ullah et al., 2012) The cumulative release profile of minocycline presents a significant release in the first 6 h period (6.7 ± 2.8 μg mL^{-1}) and another substantial release up to 48 h (13.0 ± 2.8 μg mL^{-1}). This phase is sometimes referred to as the "*second burst"* (Fredenberg et al., 2011). These results propose that minocycline was adsorbed by the polymer, even in the presence of voriconazole, sustaining a foreseen release profile.

It should be underlined that voriconazole was delivered from all scaffolds at cumulative concentrations above the MIC_{90} value of *C. albicans* (0.125 μg mL^{-1}), (Fothergill et al., 2014) right after the initial 15 min period of release. In the co-delivery system, voriconazole cumulative release profile also presented an initial burst release in the first 6 h (14.1 ± 3.2 μg mL^{-1}). These results suggest that voriconazole was also adsorbed by the polymer, even in the presence of minocycline. Further, in the co-delivery system, the voriconazole release rate till 6 h was higher (2.3±0.5 μg$mL^{-1}h^{-1}$) compared to the single delivery system (1.2±0.1 μg$mL^{-1}h^{-1}$). Minocycline exhibits a higher water

solubility (3.07 g/L) (Orti et al., 2000) in comparison to voriconazole (0.098 g/L) (Human Metabolome Database, 2022); this fact may have favored the solvent transport rate through the polymer channels and consequently the diffusion and release of voriconazole.

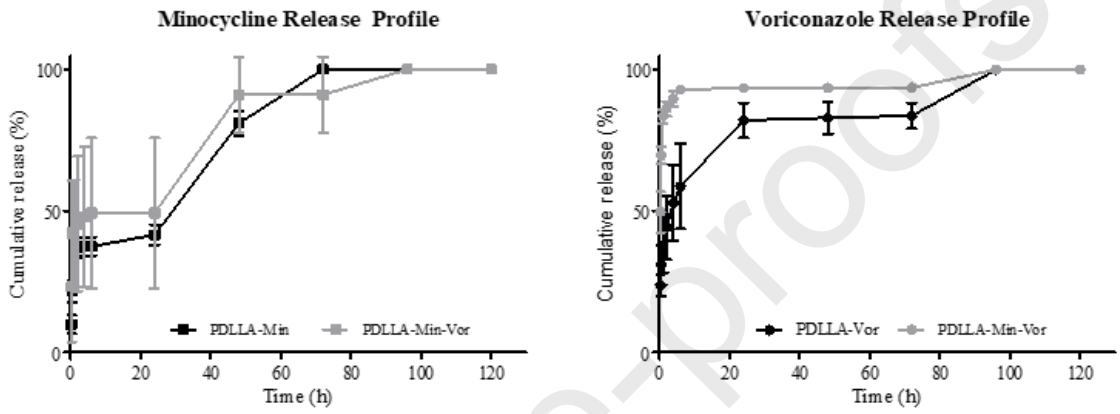

Figure 2. Comparison of release profiles of the scaffolds with different compositions (single and co-delivery). Mean ± SD (n=3).

Ultimately, the fast release of the drugs from all the PDLLA matrices within a 120 h time frame will be advantageous to prevent the development of microbial resistance. The slow liberation of drugs, often in sub-inhibitory concentrations, for an extended period of time has been suggested as a possible mechanism for the development of resistance when using local delivery devices. (Tyas et al., 2018). In view of the problem of antibiotic-resistance and translational hurdles, especially in the developmental pathways to show the clinical impact of non-antibiotic approaches, (Tyas et al., 2018) a rapidly degrading PDLLA polymer matrix combined with a rapid drug release can be advantageous to prevent the development of antibiotic resistance.

3.3 Biofilm formation assays

3.3.1. Development of biofilms models

In this study, a dual-species biofilm *in vitro* model including *S. aureus* and *C. albicans* was developed to represent part of the diversity observed in orthopedic infection. (Enz et al., 2021; Lerch et al., 2003; Li et al., 2020a; Peters et al., 2012; Zago et al., 2015) For comparison purposes, single-species biofilms were also developed. Biofilm composition, viability, morphology and structure were studied over time, in order to select the time needed to reach a mature biofilm and to understand the relationship between both microorganisms during biofilm formation *in vitro*.

The composition and viability of single- and dual-species biofilms are presented in Fig. 3. Biofilms formation was quantified using the CFUs method. To discriminate the sessile population within dual-species biofilms, selective growth media (MSA and SDA) were used. Several studies have shown that mature biofilms affect antimicrobial susceptibility, reducing their activity. (Li et al., 2020b; Trizna et al., 2020) In this sense, the biofilm formation over time was studied in order to select the time needed to reach a mature biofilm. In both cases (single- and dual-species biofilms), no significant differences in cell densities were observed over time, reaching a maximum value and stabilized biofilm production at 24 h of incubation (Fig. 3), with studies by authors. (Harriott and Noverr, 2009; Kean et al., 2017)

Regarding single-species biofilms, *S. aureus* or *C. albicans* biofilms, no significant differences were observed for cell densities over time, reaching a maximum value and stabilized biofilm production at 24 h. The bacterium *S. aureus* showed a higher ability to form a single-species biofilm (c.a. 8.50 Log_{10} CFUs mL^{-1}) compared with the fungus *C. albicans* (c.a 7.29 Log_{10} CFUs mL^{-1}) (Fig. 3).

Concerning dual-species *S. aureus* – *C. albicans* biofilm, the total and viable cell density (c.a. 8.65 Log10 CFUs mL-1, growth in TSB media) was similar to single-*S. aureus* biofilm (c.a. 8.50 Logs CFUs mL-1), and significantly higher (1-fold increased) when compared to the density of single-*C. albicans* biofilm (c.a. 7.29 Logs CFUs mL^{-1}). Within the dual-species biofilm, *S. aureus* was present in higher amounts (c.a. 8.50 Logs CFUs mL^{-1}) compared to *C. albicans* (c.a. 7.25 Logs CFUs mL^{-1}), regardless of the incubation time (Fig. 3).

No differences were found between the cell density of *S. aureus* within dual-species biofilm and single-*S. aureus* biofilm (c.a. 8.65 Logs CFUs mL^{-1}), nor between the densities of *C. albicans* within dual-species biofilm and single-*C. albicans* (c.a. 7.29 Logs CFUs mL^{-1}) biofilm (Fig. 3), indicating that both microorganisms have the ability to co-inhabit without antagonistic effect.

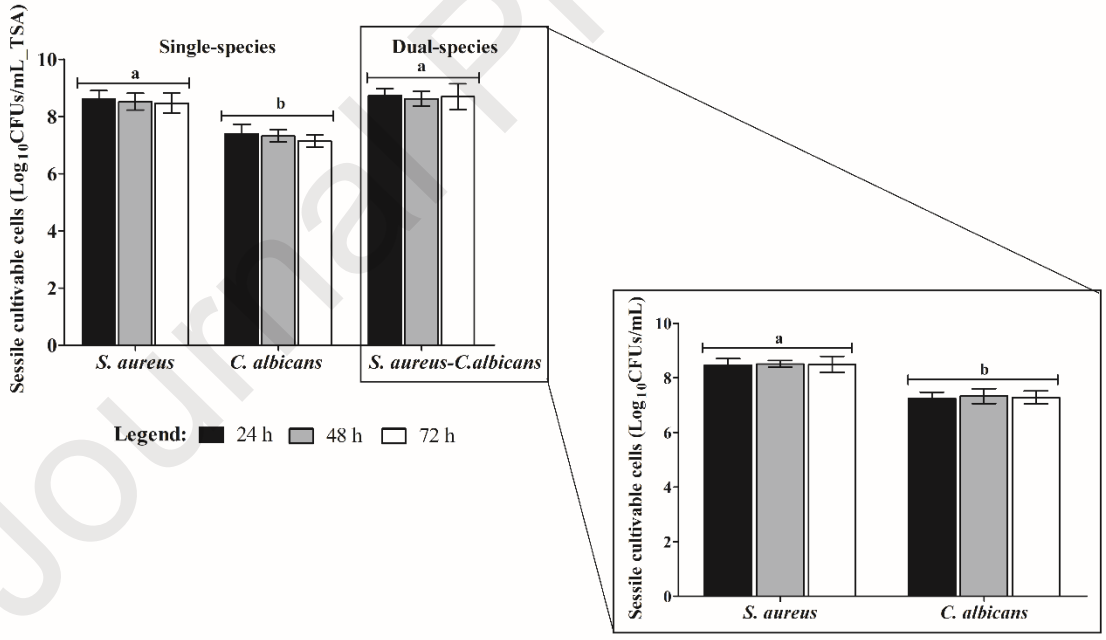

Figure 3. Quantification of composition and viability of single- and dual species biofilms, composed by *S. aureus* and *C. albicans*, during 72 h. Biofilms formation was quantified using the CFUs method and to discriminate the sessile population within dual-species biofilm, selective growth media (MSA and SDA) were used. The single-

and dual species biofilm densities were expressed in Log_{10} CFUs mL^{-1}. Different letters mean significant differences ($p < 0.05$) between time-points and biofilm groups.

SEM analysis was used to study the structure/morphology and interactions between bacterial and fungal cells in single- and dual-species biofilms (Fig. 4). SEM data shows a similar number of bacteria and/or fungus for single- or dual-species biofilms after 24, 48, and 72 h of incubation time (Fig. 4), which is in accordance with biofilm quantification data (Fig. 3). Looking at the structure and morphology of single-species biofilms, it is noticed that *S. aureus* cells were scattered almost completely on the coverslips surfaces, either as single cells or/and clusters arrangements, forming thereby a three-dimensional (3D) biofilm with mushrooms- and pillar-like structures at 24, 48 and 72 h (arrows, Fig. 4A). The single-*C. albicans* biofilm revealed a 3D structure over time, consisting of a dense mat of hyphal and yeast forms clustered in mono and multilayers (arrows, Fig. 4B). These findings show that the 24 h biofilm formation produced a mature biofilm. Concerning dual-species biofilm, it was shown that *S. aureus* cells were attached to the surface and overhead to the fungal structures, for either hyphal and yeast forms (Fig. 4 and 4C). A typical structure of a mature dual-species biofilm was observed, with the structural arrangement of multiple layers of bacterial and fungi cells embedded in extracellular polymeric substance (EPS) (circles, Fig. 4C). These results are in line with several authors who have shown that the co-culture of both microorganisms results in the formation of more rigid biofilms, where *S. aureus* is located mainly in the upper layers attached to and interspersed throughout the dense network of *C. albicans* (found mostly in the lower layers) hyphal growth. (Harriott and Noverr, 2009; Kean et al., 2017; Zago et al., 2015)

These findings show that these two microbes have a synergistic relationship co-operating with each other for biofilm formation, with the fungus *C. albicans* serving as

the base substrate for bacterium *S. aureus* colonization. (Harriott and Noverr, 2009; Kean et al., 2017; Zago et al., 2015)

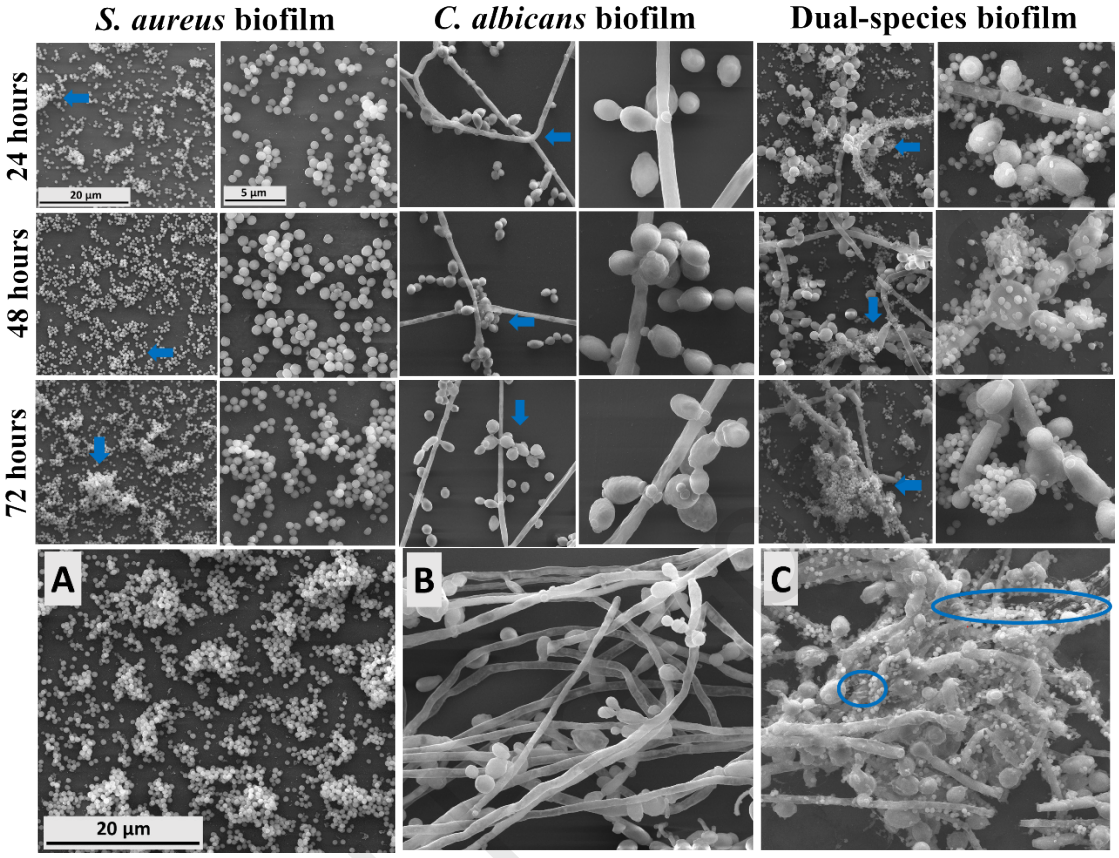

Figure 4. SEM images of single- and dual-species biofilm morphology and structure during 72 h of incubation. A) Single-*S. aureus*, B) Single-*C. albicans* and C) *S. aureus*-*C. albicans* mature biofilm. Scale bar 5 and 20 µm.

3.3.2. Scaffolds effect on mature biofilms

To evaluate the antibiofilm activity of the newly developed PDLLA scaffolds, two testing strategies were followed: i) direct contact of the scaffolds with the pre-formed biofilms and ii) effect of the solutions released at 3 time points (6, 24 and 48 h).

The antibiofilm activity of the PDLLA scaffolds loaded with minocycline and/or voriconazole after contact for 24 hours with the biofilms is depicted in Fig. 5. Regarding the single-species *S. aureus* biofilm, either PDLLA-Min or PDLLA-Min-Vor scaffolds were able to avoid biofilm formation, destroying the *S. aureus*-adherence

biofilm entirely. PDLLA-Vor scaffolds, on the other hand, had no effect on *S. aureus* biofilm formation, which was expected given that voriconazole was used as an antifungal agent.

Concerning single-species *C. albicans* biofilm, PDLLA-Vor and PDLLA-Min-Vor scaffolds reduced fungal cell densities by 97% (1.5 Logs reduction) and 96% (1.4 Logs of reduction) compared to the control PDLLA scaffolds, respectively.

In a dual-species *S. aureus*-*C. albicans* biofilm, the total number of sessile cells was not affected by PDLLA-Vor scaffolds, while PDLLA-Min and PDLLA-Min-Vor scaffolds reduced cell densities by 1.7 (97.8% reduction) and 2.8 Logs (99.8% reduction), respectively, when compared to PDLLA scaffolds (control). Looking deep inside the dual-species biofilm, it was shown that the presence of PDLLA-Vor scaffolds had no effect on *S. aureus* and *C. albicans* growth but that the presence of PDLLA-Min and PDLLA-Min-Vor scaffolds interfered with microorganisms' growth (Fig. 5). PDLLA-Min was able to totally kill the *S. aureus* population within the dual-species biofilm. Noteworthy, PDLLA-Min-Vor significantly reduced the population of *C. albicans* (1.66 Logs) by 97.6% (Fig. 5), compared to the PDLLA and PDLLA-Vor control scaffolds, most likely due to the bactericidal activity of minocycline against *S. aureus* cells in the upper layers of the biofilm, thus exposing *C. albicans* cells in the lower layers to the fungicidal action of voriconazole. Thus, the biofilm structure (Fig. 4) (Obayemi et al., 2020) can explain the differences in antibiofilm activities of PDLLA-Vor and PDLLA-Min-Vor scaffolds against *C.albicans* population within the dual-species biofilm.

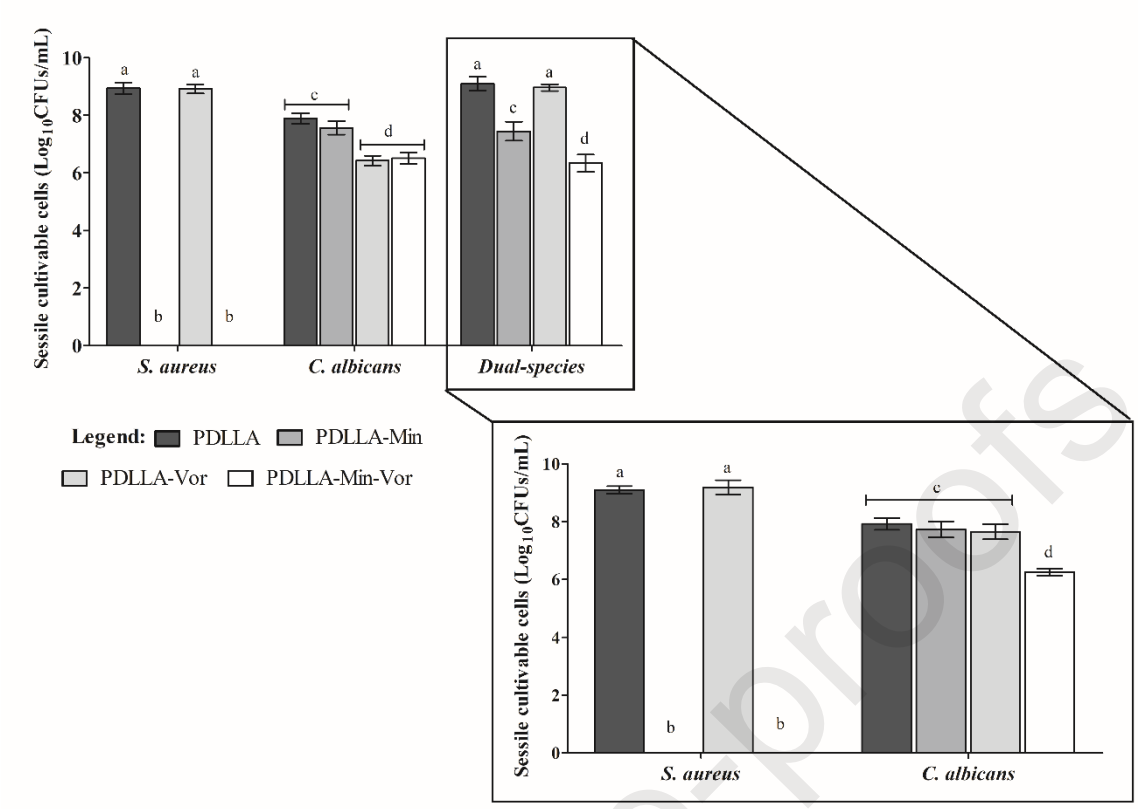

Figure 5. Antibiofilm activity (direct effect) of PDLLA, PDLLA-Min, PDLLA-Vor, and PDLLA-Min-Vor scaffolds against pre-formed single- and dual-species biofilms. PDLLA scaffolds and free-microorganisms' wells were used as positive and negative controls, respectively. The single- and dual species biofilm densities were expressed in Log_{10} CFUs mL^{-1}. Different letters mean significant differences ($p < 0.05$) between scaffolds and biofilm groups.

Moreover, the antibiofilm activity of solutions released from the scaffolds at 6, 24 and 48 h were evaluated against single- and dual-species biofilm formation (Fig. 6). As expected, single-delivery scaffolds of minocycline and voriconazole had no effect on single-species biofilm development of *C. albicans* and *S. aureus*, respectively.

Regardless of the releasing time, the minocycline solutions released from the PDLLA-Min and PDLLA-Min-Vor scaffolds were effective in preventing *S. aureus* growth in single- and dual-species biofilms (Fig. 6). Voriconazole released from PDLLA-Vor and PDLLA-Min-Vor scaffolds showed antifungal activity, but it was dependent on biofilm

composition. In the case of single-*C. albicans* biofilm, both scaffolds (PDLLA-Vor and PDLLA-Min-Vor) were able to significantly reduce biofilm density by 1.20 Logs (c.a. 91% reduction) when compared to control, regardless of the release time. Only the co-delivery solutions from PDLLA-Min-Vor scaffolds showed antifungal effectiveness in dual-species biofilms, lowering *C. albicans* densities by c.a 1.03 Logs (c.a 90% reduction).

Further, the findings imply that the antimicrobial agents loading process into the scaffolds and delivery had no effect on minocycline and voriconazole anti-biofilm activity. Besides, the results suggest that antimicrobial agents were released in sufficient amounts to reduce the biofilm formation of single- and dual-species.

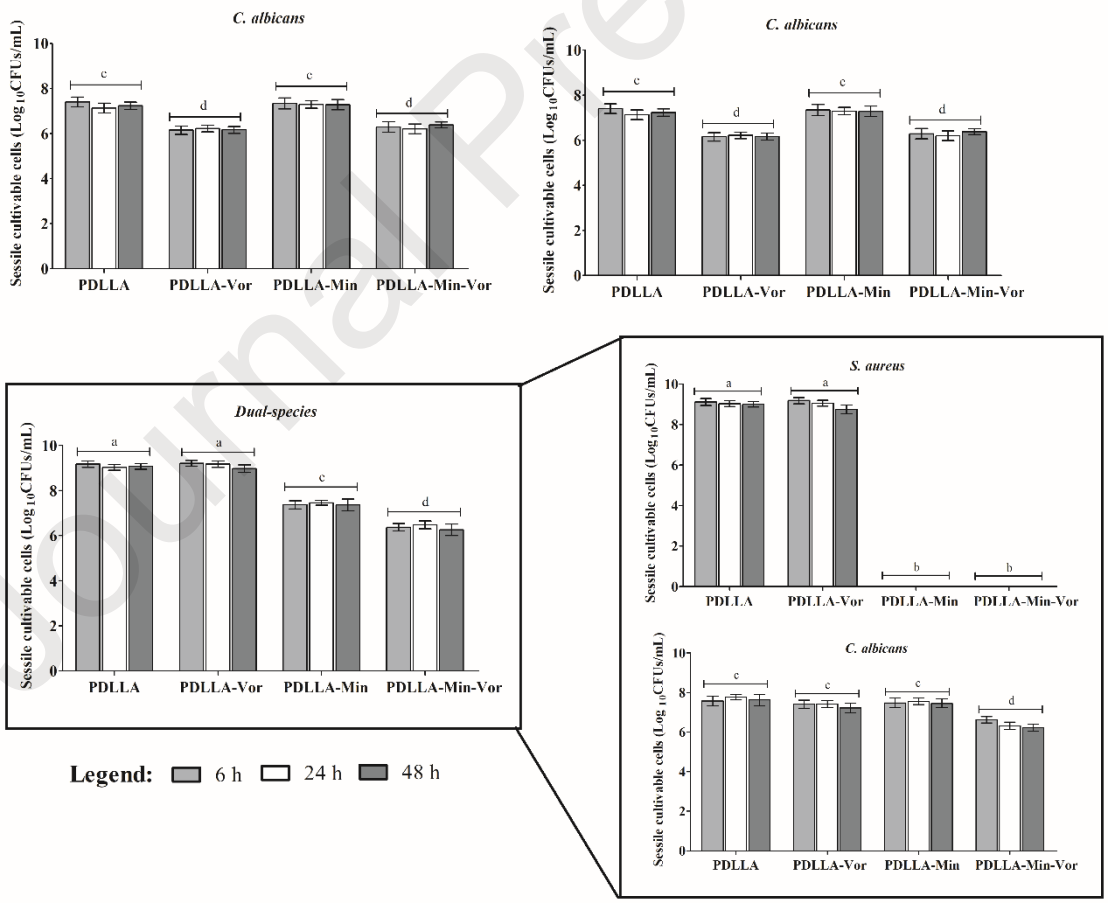

Figure 6. Antibiofilm activity of solutions released from PDLLA, PDLLA-Min, PDLLA-Vor, and PDLLA-Min-Vor scaffolds at 6, 24 and 48 h, against pre-formed single- and dual-species biofilms. Solution released from PDLLA and free microorganisms' medium were used as positive and negative controls, respectively. The sessile densities of single- and dual-species biofilms were expressed in Log_{10} CFUs mL^{-1}. Different letters mean significant differences ($p < 0.05$) between scaffolds, time-points and biofilm groups.

Overall, the obtained results emphasize that the biofilm architecture and composition can interfere with antimicrobial agents' activity. (Carolus et al., 2019; Harriott and Noverr, 2009; Kean et al., 2017) Moreover, the data suggest that the use of a co-delivery system combining antibiotic and antifungal agents could be beneficial in the control and treatment of polymicrobial-biofilm-associated infections.

3.4. Cytocompatibility and functional activity testing

When designing a novel drug loaded scaffold, the optimal concentrations for antimicrobial activity can be at the same time toxic to the bone cells and/or interfere with their differentiation and/or proliferation. In particular, minocycline may have significant toxicity effects on osteoblast cells at 0.5 mg/mL concentrations (Hatzenbuehler and Pulling, 2011) and voriconazole was cytotoxic to osteoblasts and fibroblasts, at target concentrations for local delivery (1- 20,000 μg/mL). (Schmidt et al., 2013)

Thus, it is important to evaluate the *in vitro* cytocompatibility of the PDLLA drug-loaded scaffolds. In this context, MG-63 cells, a cell line adopted to establish the cytotoxic/osteoinductive/osteoconductive effects of drugs were used (Matos et al., 2015a; Park et al., 2015). Cell proliferation and two markers of osteoblast

differentiation/proliferation (ALP activity and cellular matrix mineralization) were tested.

From the results of the Alamar Blue assay (Fig. 7), it was shown that released minocycline and voriconazole did not impair cellular proliferation, as no statistical difference was found in relation to the PDLLA control group ($p > 0.05$). Thus, drug-loaded scaffolds have no significant detrimental effect in comparison with the pristine ones.

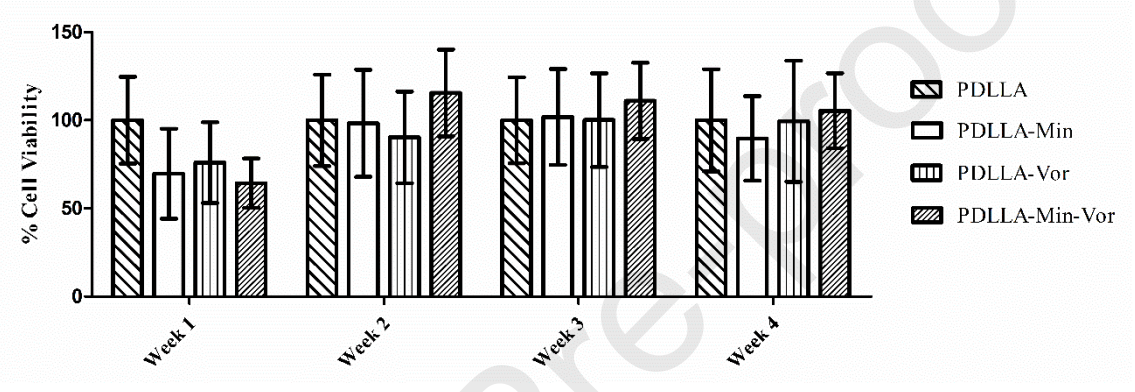

Figure 7. AlamarBlue® assay evaluating the metabolic activity of MG-63 cells when cultured with the different groups of scaffolds for 28 days (4 weeks). No significant differences ($p > 0.05$) were found in relation to PDLLA control group. Results are expressed as mean ± SD (n = 3).

Generally, ALP is an early marker of osteoblast differentiation. Thus, increased level of ALP refers to active osteoblast differentiation/proliferation. (Lee et al., 2017) In this study, the ALP activity was evaluated qualitatively (stained cells with a blue-violet color, Fig. 8A top) and quantitatively during osteoblast differentiation. ALP quantitative evaluation (Fig. 8A, graph) showed that there was no significant difference ($p > 0.05$) in the osteogenic differentiation of the cells exposed to the drug loaded scaffolds and the PDLLA control group (scaffolds without the drugs).

The Alizarin Red assay was used to evaluate calcium-rich deposits by cells in culture indicating cellular matrix mineralization (another indicator of osteoblast differentiation/proliferation). (Martin et al., 2019a) In this assay, calcium forms by chelation a calcium-alizarin complex which is orange-red in color (Fig. 8B, top). In a comparable fashion to ALP activity, there was no toxic effect of the antimicrobials in the matrix mineralization process of the osteoblasts (Fig. 8B, graph).

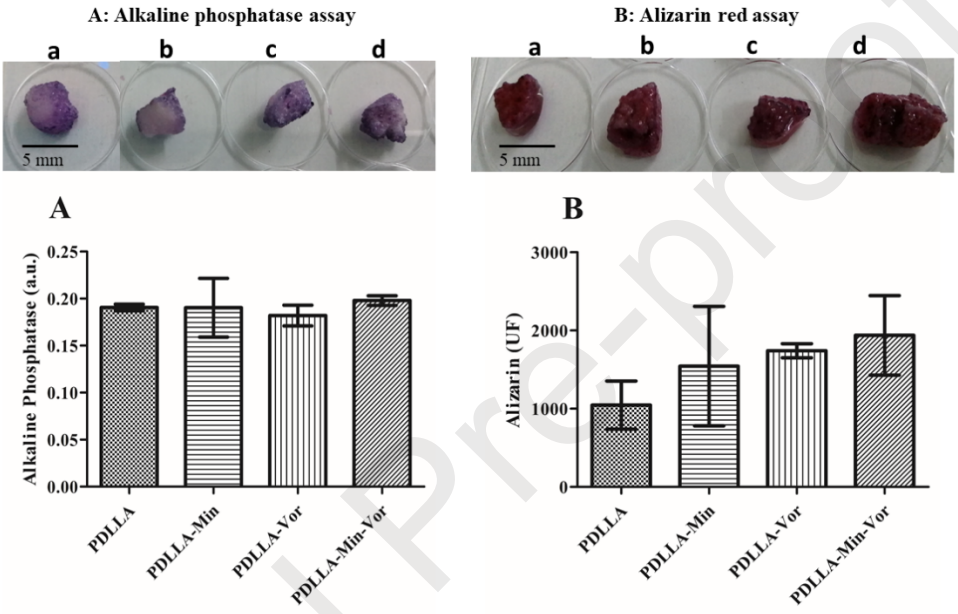

Figure 8. Alkaline phosphatase (A) and Alizarin Red (B) assays, after 28 days of MG-63 cells cultured with scaffolds. **a** corresponds to PDLLA scaffolds without the antimicrobials, **b** to PDLLA-Min, **c** to PDLLA-Vor and **d** to PDLLA-Min-Vor. Mean ± SD (n = 3). There were no statistically significant differences ($p > 0.05$) between the control (PDLLA) and the other groups.

Overall, the absence of statistically significant differences ($p > 0.05$) between the control (scaffolds without drugs) and the other groups (loaded drug scaffolds) is a clear indicator that the presence of antimicrobials in the tested concentrations does not affect the viability or the differentiation/proliferation of the osteoblasts. These results are in line with other authors, (Gomes and Fernandes, 2007) who showed that the continuous exposure to minocycline (1-10 μg/mL) caused an evident proliferation of osteoblastic-

induced bone marrow cells. Also, as for the antifungal agent, Allen et al. (Allen et al., 2015) showed that the exposure of human osteoblasts to voriconazole at 200 μg/mL (reflecting local administration) enhanced proliferation after 3 days and 7 days of treatment, while at 15 μg/mL (reflecting systemic administration) only after 7 days of treatment significant effects on proliferation were observed. In the same study, voriconazole further enhanced osteoblast ALP activity and increased intracellular calcium levels, regarding the mineralization process.

4. Conclusions

Bone infections associated with polymicrobial biofilms, namely *S-aureus – C. albicans,* pose an increasing challenge in clinical settings because of their enhanced virulence and enhanced drug tolerance often associated with bone loss. Localized drug delivery therapy aiming at dual antimicrobial effects and bone regeneration will favor the control of this disease. The scaffolds will be advantageous in comparison with the administration of the free drugs by merging a carrier and osteogenic function. In this scenario, we have developed a multifunctional PDLLA scaffold for the co-delivery of minocycline and voriconazole to address mixed infections and provide a structure for the growth of damaged bone. The developed scaffolds displayed physicochemical, and pharmaceutical properties suitable for localized antimicrobial release. Although the scaffolds' loading capacity was low, it enabled the achievement of clinically/microbiologically relevant concentrations. The PDLLA scaffolds loaded with both drugs depicted high activity against single and dual biofilm species. Supporting evidence from alkaline phosphatase expression and matrix maturation of osteoblastic cells suggests *in vitro* osteoblast differentiation/proliferation. Altogether, our *in vitro* first stage study may open paths for future works mainly dedicated to PDLLA scaffolds

as a co-delivery platform for the *S. aureus* - *C. albicans* mixed bone infections management.

Acknowledgements: The authors thank the Fundação para a Ciência e Tecnologia (FCT), Portugal for the financial support: projects UIDB/04138/2020 and UIDP/04138/2020 (iMed.Ulisboa), UIDB/00100/2020 (CQE), L. Gonçalves Principal Researcher grant (CEECIND/03143/2017), UIDB/05608/2020 and UIDP/05608/2020 (H&TRC).

Authors thank Dr. Esther Kooijman, sales support specialist from Corbion from technical assistant concerning PDLLA properties.The Graphical Abstract was created with Biorender.com.

References

Allen, K.C., Sanchez, C.J., Niece, K.L., Wenke, J.C., Akers, K.S., 2015. Voriconazole Enhances the Osteogenic Activity of Human Osteoblasts In Vitro through a Fluoride-Independent Mechanism. Antimicrob. Agents Chemother. 59, 7205–7213. https://doi.org/10.1128/AAC.00872-15

Babaei, M., Ghaee, A., Nourmohammadi, J., 2019. Poly (sodium 4-styrene sulfonate)-modified hydroxyapatite nanoparticles in zein-based scaffold as a drug carrier for vancomycin. Mater. Sci. Eng. C 100, 874–885. https://doi.org/10.1016/j.msec.2019.03.055

Babu, G.S., Raju, C.A.I., 2007. UV-spectrophotometric determination of voriconazole in bulk and its formulation. Asian J. Chem. 19, 1625–1627.

Beenken, K.E., Campbell, M.J., Ramirez, A.M., Alghazali, K., Walker, C.M., Jackson, B., Griffin, C., King, W., Bourdo, S.E., Rifkin, R., Hecht, S., Meeker, D.G., Anderson, D.E., Biris, A.S., Smeltzer, M.S., 2021. Evaluation of a bone filler scaffold for local antibiotic delivery to prevent Staphylococcus aureus infection in a contaminated bone defect. Sci. Rep. 11, 1–10. https://doi.org/10.1038/s41598-021-89830-z

Carolus, H., Van Dyck, K., Van Dijck, P., 2019. Candida albicans and Staphylococcus Species: A Threatening Twosome. Front. Microbiol. 10. https://doi.org/10.3389/fmicb.2019.02162

DeStefano, V., Khan, S., Tabada, A., 2020. Applications of PLA in modern medicine. Eng. Regen. 1, 76–87. https://doi.org/10.1016/j.engreg.2020.08.002

Doty, H.A., Leedy, M.R., Courtney, H.S., Haggard, W.O., Bumgardner, J.D., 2014. Composite chitosan and calcium sulfate scaffold for dual delivery of vancomycin and recombinant human bone morphogenetic protein-2. J. Mater. Sci. Mater. Med. 25, 1449–1459. https://doi.org/10.1007/s10856-014-5167-7

Du, L., Yang, S., Li, W., Li, H., Feng, S., Zeng, R., Yu, B., Xiao, L., Nie, H.-Y., Tu, M., 2017. Scaffold composed of porous vancomycin-loaded poly(lactide- co -glycolide) microspheres: A controlled-release drug delivery system with shape-memory effect. Mater. Sci. Eng. C 78, 1172–1178. https://doi.org/10.1016/j.msec.2017.04.099

Enz, A., Mueller, S.C., Warnke, P., Ellenrieder, M., Mittelmeier, W., Klinder, A., 2021. Periprosthetic Fungal Infections in Severe Endoprosthetic Infections of the Hip and Knee Joint—A Retrospective Analysis of a Certified Arthroplasty Centre of Excellence. J. Fungi 7, 404. https://doi.org/10.3390/jof7060404

Fanaei Pirlar, R., Emaneini, M., Beigverdi, R., Banar, M., B. van Leeuwen, W., Jabalameli, F., 2020. Combinatorial effects of antibiotics and enzymes against dual-species Staphylococcus aureus and Pseudomonas aeruginosa biofilms in the wound-like medium. PLoS One 15, e0235093. https://doi.org/10.1371/journal.pone.0235093

Farokhi, M., Mottaghitalab, F., Shokrgozar, M.A., Ou, K.-L., Mao, C., Hosseinkhani, H., 2016. Importance of dual delivery systems for bone tissue engineering. J. Control. Release 225, 152–169. https://doi.org/10.1016/j.jconrel.2016.01.033

Ferreira, I.S., Bettencourt, A.F., Gonçalves, L.M.D., Kasper, S., Bétrisey, B., Kikhney, J., Moter, A., Trampuz, A., Almeida, A.J., 2015. Activity of daptomycin-and vancomycin-loaded poly-epsilon-caprolactone microparticles against mature staphylococcal biofilms. Int. J. Nanomedicine 10, 4351.

Flurin, L., Raval, Y.S., Mohamed, A., Greenwood-Quaintance, K.E., Cano, E.J., Beyenal, H., Patel, R., 2021. An integrated hocl-producing e-scaffold is active against monomicrobial and polymicrobial biofilms. Antimicrob. Agents Chemother. 65, 1–12. https://doi.org/10.1128/AAC.02007-20

Fothergill, A.W., Sutton, D.A., McCarthy, D.I., Wiederhold, N.P., 2014. Impact of new antifungal breakpoints on antifungal resistance in Candida species. J. Clin. Microbiol. 52, 994–997. https://doi.org/10.1128/JCM.03044-13

Fredenberg, S., Wahlgren, M., Reslow, M., Axelsson, A., 2011. The mechanisms of drug release in poly(lactic-co-glycolic acid)-based drug delivery systems - A review. Int. J. Pharm. 415, 34–52. https://doi.org/10.1016/j.ijpharm.2011.05.049

Gomes, P.S., Fernandes, M.H., 2007. Effect of therapeutic levels of doxycycline and minocycline in the proliferation and differentiation of human bone marrow osteoblastic cells. Arch. Oral Biol. 52, 251–259. https://doi.org/10.1016/j.archoralbio.2006.10.005

Harriott, M.M., Noverr, M.C., 2009. Candida albicans and Staphylococcus aureus Form Polymicrobial Biofilms: Effects on Antimicrobial Resistance. Antimicrob. Agents Chemother. 53, 3914–3922. https://doi.org/10.1128/AAC.00657-09

Hatzenbuehler, J. (Maine M.C., Pulling, T. (Maine M.C., 2011. Diagnosis and management of osteomyelitis. Am. Fam. Physician 84, 1027–1033.

Huang, X., Brazel, C.S., 2001. On the importance and mechanisms of burst release in matrix-controlled drug delivery systems. J. Control. Release 73, 121–136. https://doi.org/10.1016/S0168-3659(01)00248-6

Human Metabolome Database, 2022. Metabocard for Voriconazole (HMDB0014720) [WWW Document]. URL https://hmdb.ca/metabolites/HMDB0014720

Kean, R., Rajendran, R., Haggarty, J., Townsend, E.M., Short, B., Burgess, K.E., Lang, S., Millington, O., Mackay, W.G., Williams, C., Ramage, G., 2017. Candida albicans Mycofilms Support Staphylococcus aureus Colonization and Enhances Miconazole Resistance in Dual-Species Interactions. Front. Microbiol. 8. https://doi.org/10.3389/fmicb.2017.00258

Leal, C.V., Santos Almeida, R., Dávila, J.L., Domingues, J.A., Hausen, M.A., Duek, E.A.R., D'Ávila, M.A., 2019. Characterization and in vitro evaluation of electrospun aligned-fiber membranes of poly(L -co- D , L -lactic acid). J. Appl. Polym. Sci. 136, 47657. https://doi.org/10.1002/app.47657

Lee, J.-M., Kim, M.-G., Byun, J.-H., Kim, G.-C., Ro, J.-H., Hwang, D.-S., Choi, B.-B., Park, G.-C., Kim, U.-K., 2017. The effect of biomechanical stimulation on osteoblast differentiation of human jaw periosteum-derived stem cells. Maxillofac. Plast. Reconstr. Surg. 39, 7. https://doi.org/10.1186/s40902-017-0104-6

Lerch, K., Kalteis, T., Schubert, T., Lehn, N., Grifka, J., 2003. Prosthetic joint infections with osteomyelitis due to Candida albicans. Mycoses 46, 462–466. https://doi.org/10.1046/j.0933-7407.2003.00928.x

Li, X., Xu, J., Filion, T.M., Ayers, D.C., Song, J., 2013. pHEMA-nHA Encapsulation and Delivery of Vancomycin and rhBMP-2 Enhances its Role as a Bone Graft Substitute. Clin. Orthop. Relat. Res. 471, 2540–2547. https://doi.org/10.1007/s11999-012-2644-5

Li, Y., Xiao, P., Wang, Y., Hao, Y., 2020a. Mechanisms and control measures of mature biofilm resistance to antimicrobial agents in the clinical context. ACS Omega 5, 22684–22690. https://doi.org/10.1021/acsomega.0c02294

Li, Y., Xiao, P., Wang, Y., Hao, Y., 2020b. Mechanisms and Control Measures of Mature Biofilm Resistance to Antimicrobial Agents in the Clinical Context. ACS Omega 5, 22684–22690. https://doi.org/10.1021/acsomega.0c02294

Martin, V., Anjos, I., Saraiva, A.S., Zuza, E., Goncalves, L., Alves, M., Santos, C., Ribeiro, I., Bettencourt, A., 2019a. Composite scaffolds for bone regeneration and infection control, in: 2019 IEEE 6th Portuguese Meeting on Bioengineering (ENBENG). IEEE, pp. 1–4. https://doi.org/10.1109/ENBENG.2019.8692450

Martin, V., Ribeiro, I.A.C., Alves, M.M., Gonçalves, L., Almeida, A.J., Grenho, L., Fernandes, M.H., Santos, C.F., Gomes, P.S., Bettencourt, A.F., 2019b. Understanding intracellular trafficking and anti-inflammatory effects of minocycline chitosan-nanoparticles in human gingival fibroblasts for periodontal disease treatment. Int. J. Pharm. 572, 118821.

https://doi.org/10.1016/j.ijpharm.2019.118821

Matos, A.C., Marques, C.F., Pinto, R. V., Ribeiro, I.A.C., Gonçalves, L.M., Vaz, M.A., Ferreira, J.M.F., Almeida, A.J., Bettencourt, A.F., 2015a. Novel doped calcium phosphate-PMMA bone cement composites as levofloxacin delivery systems. Int. J. Pharm. 490, 200–208. https://doi.org/10.1016/j.ijpharm.2015.05.038

Matos, A.C., Ribeiro, I.A.C., Guedes, R.C., Pinto, R., Vaz, M.A., Gonçalves, L.M., Almeida, A.J., Bettencourt, A.F., 2015b. Key-properties outlook of a levofloxacin-loaded acrylic bone cement with improved antibiotic delivery. Int. J. Pharm. 485, 317–328. https://doi.org/10.1016/j.ijpharm.2015.03.035

McLaren, J.S., White, L.J., Cox, H.C., Ashraf, W., Rahman, C. V., Blunn, G.W., Goodship, A.E., Quirk, R.A., Shakesheff, K.M., Bayston, R., Scammell, B.E., 2014. A biodegradable antibiotic-impregnated scaffold to prevent osteomyelitis in a contaminated in vivo bone defect model. Eur. Cells Mater. 27, 332–349. https://doi.org/10.22203/eCM.v027a24

Miller, R.B., McLaren, A.C., Pauken, C., Clarke, H.D., McLemore, R., 2013. Voriconazole Is Delivered From Antifungal-Loaded Bone Cement. Clin. Orthop. Relat. Res. 471, 195–200. https://doi.org/10.1007/s11999-012-2463-8

Mouriño, V., Boccaccini, A.R., 2010. Bone tissue engineering therapeutics: controlled drug delivery in three-dimensional scaffolds. J. R. Soc. Interface 7, 209–227. https://doi.org/10.1098/rsif.2009.0379

Obayemi, J.D., Jusu, S.M., Salifu, A.A., Ghahremani, S., Tadesse, M., Uzonwanne, V.O., Soboyejo, W.O., 2020. Degradable porous drug-loaded polymer scaffolds for localized cancer drug delivery and breast cell/tissue growth. Mater. Sci. Eng. C 112, 110794. https://doi.org/10.1016/j.msec.2020.110794

Orti, V., Audran, M., Gibert, P., Bougard, G., Bressolle, F., 2000. High-performance liquid chromatographic assay for minocycline in human plasma and parotid saliva. J. Chromatogr. B Biomed. Sci. Appl. 738, 357–365. https://doi.org/10.1016/S0378-4347(99)00547-2

Park, K.-W., Yun, Y.-P., Kim, S., Song, H.-R., 2015. The Effect of Alendronate Loaded Biphasic Calcium Phosphate Scaffolds on Bone Regeneration in a Rat Tibial

Defect Model. Int. J. Mol. Sci. 16, 26738–26753. https://doi.org/10.3390/ijms161125982

Peters, B.M., Jabra-Rizk, M.A., O'May, G.A., William Costerton, J., Shirtliff, M.E., 2012. Polymicrobial interactions: Impact on pathogenesis and human disease. Clin. Microbiol. Rev. 25, 193–213. https://doi.org/10.1128/CMR.00013-11

Qu, Y., Locock, K., Verma-Gaur, J., Hay, I.D., Meagher, L., Traven, A., 2016. Searching for new strategies against polymicrobial biofilm infections: guanylated polymethacrylates kill mixed fungal/bacterial biofilms. J. Antimicrob. Chemother. 71, 413–421. https://doi.org/10.1093/jac/dkv334

Schmidt, K., McLaren, A., Pauken, C., McLemore, R., 2013. Voriconazole Is Cytotoxic at Locally Delivered Concentrations: A Pilot Study. Clin. Orthop. Relat. Res. 471, 3165–3170. https://doi.org/10.1007/s11999-013-2860-7

Silva, E., Vasconcellos, L.M.R. de, Rodrigues, B.V.M., dos Santos, D.M., Campana-Filho, S.P., Marciano, F.R., Webster, T.J., Lobo, A.O., 2017. PDLLA honeycomb-like scaffolds with a high loading of superhydrophilic graphene/multi-walled carbon nanotubes promote osteoblast in vitro functions and guided in vivo bone regeneration. Mater. Sci. Eng. C 73, 31–39. https://doi.org/10.1016/j.msec.2016.11.075

Sreeja, S., Muraleedharan, C.V., Varma, P.R.H., Sailaja, G.S., 2020. Surface-transformed osteoinductive polyethylene terephthalate scaffold as a dual system for bone tissue regeneration with localized antibiotic delivery. Mater. Sci. Eng. C 109, 110491. https://doi.org/10.1016/j.msec.2019.110491

Tan, J., Jiang, S., Tan, L., Shi, H., Yang, L., Sun, Y., Wang, X., 2021. Antifungal Activity of Minocycline and Azoles Against Fluconazole-Resistant Candida Species. Front. Microbiol. 12. https://doi.org/10.3389/fmicb.2021.649026

Trizna, E.Y., Yarullina, M.N., Baidamshina, D.R., Mironova, A. V., Akhatova, F.S., Rozhina, E. V., Fakhrullin, R.F., Khabibrakhmanova, A.M., Kurbangalieva, A.R., Bogachev, M.I., Kayumov, A.R., 2020. Bidirectional alterations in antibiotics susceptibility in Staphylococcus aureus—Pseudomonas aeruginosa dual-species biofilm. Sci. Rep. 10, 14849. https://doi.org/10.1038/s41598-020-71834-w

Tyas, B., Marsh, M., Oswald, T., Refaie, R., Molyneux, C., Reed, M., 2018. Antibiotic resistance profiles of deep surgical site infections in hip hemiarthroplasty; comparing low dose single antibiotic versus high dose dual antibiotic impregnated cement. J. Bone Jt. Infect. 3, 123–129. https://doi.org/10.7150/jbji.22192

Ullah, Farhat, Malik, S.A., Ahmed, J., Ullah, Farman, Shah, S.M., Ayaz, M., Hussain, S., Khatoon, L., 2012. Investigation of the genetic basis of tetracycline resistance in Staphylococcus aureus from Pakistan. Trop. J. Pharm. Res. 11, 925–931. https://doi.org/10.4314/tjpr.v11i6.8

Üstündağ Okur, N., Çağlar, E.Ş., YOZGATLI, V., 2016. Development and Validation of an Hplc Method for Voriconazole Active Substance in Bulk and its Pharmaceutical Formulation. MARMARA Pharm. J. 20, 79. https://doi.org/10.12991/mpj.20162076793

Van Dyck, K., Pinto, R.M., Pully, D., Van Dijck, P., 2021a. Microbial interkingdom biofilms and the quest for novel therapeutic strategies. Microorganisms 9, 1–22. https://doi.org/10.3390/microorganisms9020412

Van Dyck, K., Pinto, R.M., Pully, D., Van Dijck, P., 2021b. Microbial Interkingdom Biofilms and the Quest for Novel Therapeutic Strategies. Microorganisms 9, 412. https://doi.org/10.3390/microorganisms9020412

Wang, C., Lai, J., Li, K., Zhu, S., Lu, B., Liu, J., Tang, Y., Wei, Y., 2021. Cryogenic 3D printing of dual-delivery scaffolds for improved bone regeneration with enhanced vascularization. Bioact. Mater. 6, 137–145. https://doi.org/10.1016/j.bioactmat.2020.07.007

Xiao, L., Wang, B., Yang, G., Gauthier, M., 2012. Poly(Lactic Acid)-Based Biomaterials: Synthesis, Modification and Applications, in: Biomedical Science, Engineering and Technology. InTech. https://doi.org/10.5772/23927

Yang, Y., Qiu, X., Sun, Y., Wang, Y., Wang, J., Li, Y., Liu, C., 2018. Development of bioabsorbable polylactide membrane with controllable hydrophilicity for adjustment of cell behaviours. R. Soc. Open Sci. 5, 170868. https://doi.org/10.1098/rsos.170868

Zago, C.E., Silva, S., Sanitá, P.V., Barbugli, P.A., Dias, C.M.I., Lordello, V.B.,

Vergani, C.E., 2015. Dynamics of biofilm formation and the Interaction between Candida albicans and methicillin-susceptible (MSSA) and -resistant Staphylococcus aureus (MRSA). PLoS One 10, 1–15. https://doi.org/10.1371/journal.pone.0123206

HIGHLIGHTS

- Minocycline and voriconazole-loaded PDLLA porous sponge-like scaffolds were successfully prepared by solvent casting technique.
- Analysis of drug release tests confirmed the co-delivery of both drugs, mainly by Fickian diffusion.
- *S. aureus* and *C. albicans* showed a synergic cooperation in dual-species biofilm formation.
- PDLLA scaffolds loaded with minocycline and voriconazole showed anti-bacterial and antifungal effectiveness in dual-species biofilms.
- *In vitro* tests revealed adequate cytocompatibility and osteoblast proliferation/growth support for the minocycline and voriconazole-loaded PDLLA scaffolds.

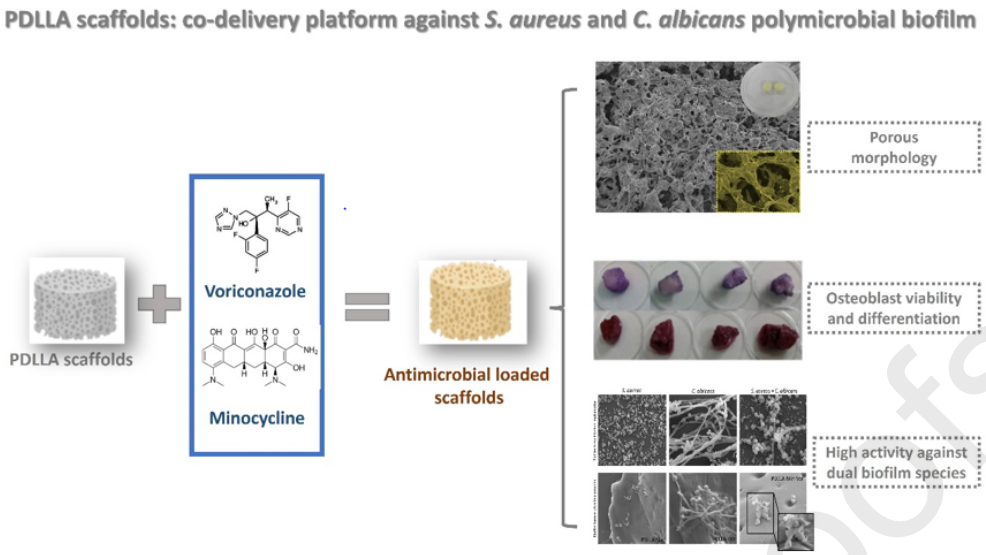

CRediT author statement

M. Zegre: Investigation, Methodology, Original draft preparation. **J. Barros**: Investigation, Methodology, Original draft preparation. **I.A.C. Ribeiro**: Methodology, Validation, Writing- Reviewing and Editing. C. Santos: Investigation, Methodology, Writing- Original draft preparation. **L.A. Caetano**: Supervision, Writing- Reviewing and Editing. **L. Gonçalves**: Investigation, Validation, Supervision. **F.J. Monteiro**: Resource, Supervision, Writing- Reviewing and Editing. **M.P. Ferraz**: Conceptualization, Supervision, Writing- Reviewing and Editing. **A. Bettencourt**: Conceptualization, Supervision, Writing- Reviewing and Editing, Project administration.